Supplementary material

4D Imaging and Diffraction Dynamics of Single-Particle Phase Transition in Heterogeneous Ensembles

Haihua Liu,[1] Oh-Hoon Kwon,[1,3] Jau Tang,[2] and Ahmed H. Zewail[1,*]

[1]*Physical Biology Center for Ultrafast Science and Technology, Arthur Amos Noyes Laboratory of Chemical Physics, California Institute of Technology, Pasadena, CA 91125, USA*

[2]*Research Center for Applied Sciences, Academia Sinica, Taipei, 11529, Taiwan.*

Present Address:

[3] Department of Chemistry, School of Nano-Bioscience and Chemical Engineering, Ulsan National Institute of Science and Technology (UNIST), Ulsan 689-798, Republic of Korea

Thermal hysteresis loop study of single VO_2 nanoparticles

The heating and cooling thermal hysteresis loops were experimentally determined in order to investigate the phase transition of single vanadium dioxide nanoparticles. Polycrystalline VO_2 films were grown on grapheme substrate via a sol-gel method. Fig. S1(A) shows one typical bright field image of an ensemble of vanadium dioxide nanocrystals. Fig. S1(B) is one selected area electron diffraction (SAED) pattern obtained from the same area as in Fig. S1(A), which

indicates that the nanoparticles are oriented randomly. Figs.S1(C-E) shows the corresponding dark field images of the particles marked by a, b, c on Fig. S1(A), respectively.

The heating and cooling hysteresis loops of the SAED patterns were recorded using a Gatan 626 Cyro holder at a step of 2.5^{o}C from 25^{o}C to 90^{o}C in the transmission mode of UEM2 at Caltech. The recorded SAED patterns were then aligned to eliminate the image drift during data collection. The single-particle selectivity is obtained by using conical scanning dark field imaging method. The conical scanning dark field imaging here was carried out at a step of 2^{o} in β direction along 16 different Debye-Scherrer rings in the α direction. The Bragg diffraction spots marked by 1, 2, 3 in Fig. S1(B) are connected with the grains denoted by a, b, c on Fig. S1(A), respectively.

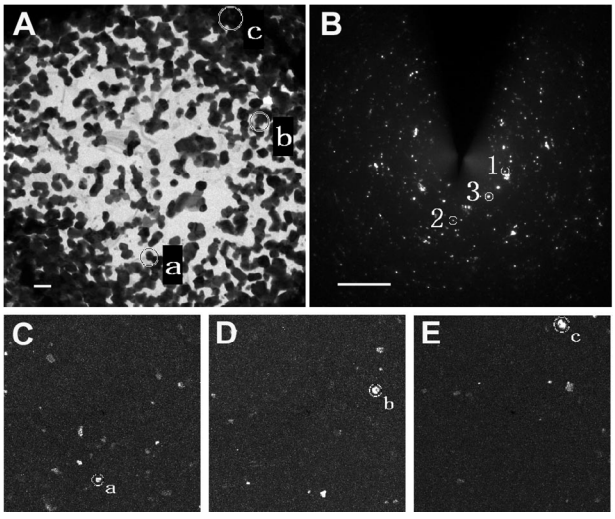

Fig. S1(A) The bright field image of vanadium dioxide. Scale bar, 300 nm. (B) Selected area electron diffraction pattern of vanadium dioxide. Scale bar, 5 nm^{-1}. (C-E) The corresponding dark field images of the particles as marked by a, b, c, respectively.

The intensity change of Bragg diffraction peaks marked by 1, 2, 3 during the hysteresis loops are represented in Figs. S2(A-C), respectively. Fig. S2(D) shows the hysteresis width decreases with the increase in particle size, which indicates that the size plays an important role in the phase transition of vanadium dioxide nanocrystals. The insert in Fig. S2(D) depicts the measured threshold temperature for phase transition in VO_2 with particle size and during the heating and cooling cycle. From the hysteresis loop profiles, the threshold temperature for phase transition in VO_2 upon heating is almost unchanged for different particle sizes. However, the phase transition upon cooling occurs at lower temperatures with the decrease in particle size.

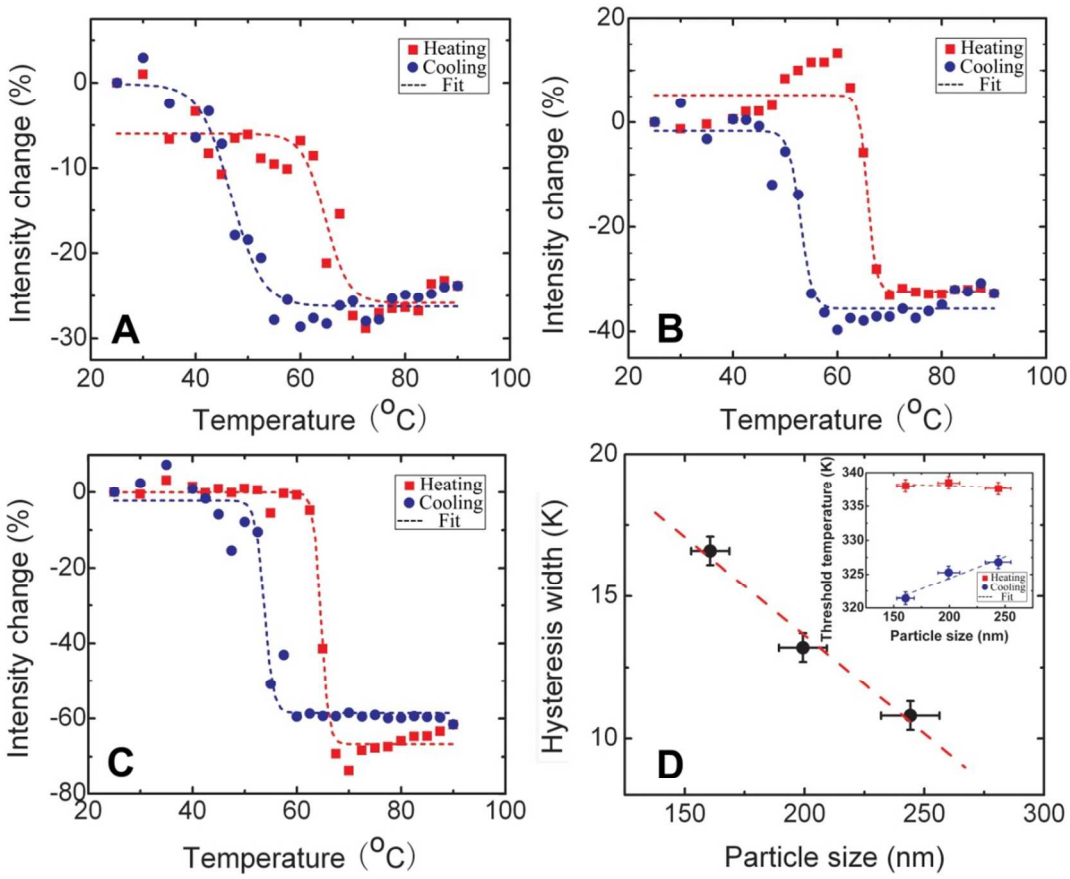

Fig. S2. Thermal hysteresis loops of Bragg diffraction intensity of the spots shown in Fig. S1(B) in vanadium dioxide (A-C). The fits (dash lines) were obtained by using two sigmoidal functions.

(A) Particle a: size, 160 nm, hysteresis width, 16.6 ^{o}C; (B) Particle b: size, 199 nm, hysteresis width, 13.2 ^{o}C; (C) Particle c: size, 244 nm, hysteresis width, 10.8 ^{o}C; (D) The hysteresis width as a function of the particle size. The width decreases as the increasing particle size increases. The insert in (D) shows the threshold temperature for phase transition during heating and cooling cycle. The dash lines are the linear fits.

Cooling rate of the VO_2 nanocrystals and size dependence

Here we discuss the size dependence of the cooling rate of VO_2 nanocrystals as caused by the heat transfer from the VO_2 grain to the graphene substrate and the underneath copper wire grids in the UEM experiments. Because of the thermal conductivity of either grapheme or copper is several orders of magnitude higher than that of VO_2, one can simply assumes that the graphene substrate is a "perfect" heat sink. The temperature change with time of a given VO_2 grain of the tetragonal phase can be expressed as,

$$C_{P_t}\rho_t V\frac{d}{dt}T_t = -c\kappa_t A(T_t - 298) \quad \text{or} \quad \frac{d}{dt}T_t = -\frac{c\kappa_t A}{C_{P_t}\rho_t V}(T-298)_t, \tag{1a}$$

and similarly for the monolithic phase as,

$$C_{P,m}\rho_m V\frac{d}{dt}T_m = -cA\kappa_m(T_m - 298) \quad \text{or} \quad \frac{d}{dt}T_m = -\frac{c\kappa_m A}{C_{P_m}\rho_m V}(T_m - 298) \tag{1b}$$

where κ is the thermal conductivity, V is the grain volumn L^3 and A is the contact area which equals to L^2 of the cube-shaped grain. Therefore, according to dimension analysis, the effective cooling rates are given by

$$\gamma_m = \frac{c\kappa_m}{C_{Pm}\rho_m L} \quad \text{and} \quad \gamma_t = \frac{c\kappa_t}{C_{Pt}\rho_t L} \tag{2}$$

Eq. (2) indicates that the cooling rate is size dependent and varies for different phases. Even the temperature raised by laser heating is higher for a smaller grain, however, due to its much greater cooling rate, it is faster to be cooled down to reach the recrystallization temperature that represents the phase transition from the tetragonal phase back to the monolithic phase. This result of size-dependent cooling rate is important for the findings reported here.